Analysis of the electrical properties of Cr/n-BaSi2 Schottky junction and n-BaSi2/p-Si heterojunction diodes for solar cell applications

Weijie Du, Masakazu Baba, Kaoru Toko, Kosuke O. Hara, Kentaro Watanabe, Takashi Sekiguchi, Noritaka Usami, and Takashi Suemasu

Articles you may be interested in

Transport mechanisms and effective Schottky barrier height of ZnO/a-Si:H and ZnO/c-Si:H heterojunction solar cells
J. Appl. Phys. **114**, 184505 (2013); 10.1063/1.4831661

Electrical transport properties of isolated carbon nanotube/Si heterojunction Schottky diodes
Appl. Phys. Lett. **103**, 193111 (2013); 10.1063/1.4829155

On the electrical behavior of V2O5/4H-SiC Schottky diodes
J. Appl. Phys. **113**, 224503 (2013); 10.1063/1.4809543

Modified, semiconducting graphene in contact with a metal: Characterization of the Schottky diode
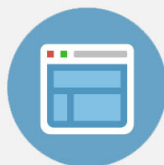Appl. Phys. Lett. **97**, 163101 (2010); 10.1063/1.3495777

Graphite based Schottky diodes formed on Si, GaAs, and 4H-SiC substrates
Appl. Phys. Lett. **95**, 222103 (2009); 10.1063/1.3268788

CrossMark
click for updates

Analysis of the electrical properties of Cr/n-BaSi₂ Schottky junction and n-BaSi₂/p-Si heterojunction diodes for solar cell applications

Weijie Du,[1] Masakazu Baba,[1] Kaoru Toko,[1] Kosuke O. Hara,[2] Kentaro Watanabe,[1,3] Takashi Sekiguchi,[3] Noritaka Usami,[2,4] and Takashi Suemasu[1,4]

[1]*Institute of Applied Physics, University of Tsukuba, Tsukuba, Ibaraki 305-8573, Japan*
[2]*Graduate School of Engineering, Nagoya University, Chikusa-ku, Nagoya 464-8603, Japan*
[3]*National Institute for Materials Science, Tsukuba, Ibaraki 305-0044, Japan*
[4]*Core Research for Evolutional Science and Technology, Japan Science and Technology Agency, Chiyoda, Tokyo 102-0075, Japan*

Current status and future prospects towards BaSi₂ pn junction solar cells are presented. As a preliminary step toward the formation of BaSi₂ homojunction diodes, diodes with a Cr/n-BaSi₂ Schottky junction and an n-BaSi₂/p-Si hetero-junction have been fabricated to investigate the electrical properties of the n-BaSi₂. Clear rectifying properties were observed in the current density versus voltage characteristics in both diodes. From the capacitance-voltage measurements, the build-in potential, V_D, was 0.53 V in the Cr/n-BaSi₂ Schottky junction diode, and the Schottky barrier height was 0.73 eV calculated from the thermoionic emission theory; the V_D was about 1.5 V in the n-BaSi₂/p-Si hetero-junction diode, which was consistent with the difference in the Fermi level between the n-BaSi₂ and the p-Si. © *2014 AIP Publishing LLC.* [http://dx.doi.org/10.1063/1.4882117]

I. INTRODUCTION

In recent years, thin-film solar cells such as Cu(In,Ga)Se₂, Cu₂ZnSnS₄, and CdTe have been attracting so much attention due to their high efficiency and low cost.[1–5] We think that barium disilicide (BaSi₂) could be another candidate material.[6,7] The band gap of BaSi₂ is approximately 1.3 eV that matches the solar spectrum better than crystalline Si.[8,9] Both theoretical and experimental researches revealed that BaSi₂ has a very large absorption coefficient of over $3 \times 10^4 \, cm^{-1}$ for photon energies greater than 1.5 eV.[10,11] We have already grown high-quality BaSi₂ epitaxial layers on both Si(111) and Si(001) substrates even though BaSi₂ has an orthorhombic crystal structure.[12–15] We have further formed polycrystalline BaSi₂ layers on ⟨111⟩-oriented Si films prepared on SiO₂ using an Al-induced crystallization method.[16] Besides, the undoped n-BaSi₂ has a large minority-carrier (holes) diffusion length (∼10 μm) and thereby a long minority carrier lifetime (>10 μs).[17–19] These results have suggested that BaSi₂ is a very promising material for thin-film solar cell applications. To form BaSi₂ homojunction diodes, the properties of BaSi₂ thin-films doped with impurities such as Cu, Ag, Sb, P, As, In, Al, and B have also been investigated.[20–26] Among these elements, Sb and B were proved to be the suitable candidates for n⁺-BaSi₂ and p⁺-BaSi₂, respectively. Their diffusion coefficients are another important parameter that should be taken into account. Most impurities, such as Al, Sb, and As, except B have large diffusion coefficients in BaSi₂ layers.[27–29]

As a next step toward forming a BaSi₂ homojunction diode on a Si substrate, we need to investigate the electrical properties of an undoped n-type BaSi₂ film, which is to be an active layer in a solar cell. Due to the small electron affinity of BaSi₂ (3.2 eV), band offsets exist at the BaSi₂/Si interface,[30,31] that is, 0.8 eV for the conduction band, and 0.6 eV for the valence band. These values are predicted from the electron affinities of BaSi₂ and Si. The band offsets block the photocurrent flowing across the BaSi₂/Si interface. An Sb-doped n⁺-BaSi₂/p⁺-Si tunnel junction (TJ) solved this problem.[32–34] Recently, we have achieved large photocurrent corresponding to the internal quantum efficiency exceeding 70% for the 400 nm-thick undoped n-BaSi₂ layer grown on the Sb-doped n⁺-BaSi₂/p⁺-Si TJ.[35] The remaining process is the formation of p-BaSi₂ layer on the undoped n-BaSi₂ layer to complete the BaSi₂ homojunction diode. However, there has been no report even on the built-in potential, V_D, in a BaSi₂/Si heterojunction diode or in a metal/BaSi₂ Schottky junction diode, which is one of the most fundamental electrical properties in semiconductors. In an n-BaSi₂/p-Si heterojunction diode, for example, the V_D is given ideally by the difference in work function between the n-BaSi₂ and p-Si. Assuming that the effective density of states of conduction band, N_C, is approximately $2.6 \times 10^{19} \, cm^{-3}$ from the effective mass tensors of electron in BaSi₂,[11] the separation of the bottom of the conduction band, E_C, from the Fermi level, E_F, that is $E_C - E_F$, can be estimated using the value of electron concentration. Thus, the work function of the n-BaSi₂ can be calculated. The same is true for the p-Si. In this article, we grew an undoped n-BaSi₂ layer on a p-Si(111) for that purpose. An undoped n-BaSi₂ layer was also formed on the TJ, and a Schottky junction was formed on top of the n-BaSi₂ with Cr for comparison. Then, we measured the current-density versus voltage (J-V) and capacitance-voltage (C-V) characteristics of the above two diodes and compare their V_D's with those predicted from their work functions.

II. EXPERIMENTAL

An ion-pumped molecular beam epitaxy (MBE) system was used for the growth of samples. For the Schottky junction diode, the p⁺-Si ($\rho \leq 0.01 \, \Omega \cdot cm$) substrate was adopted.

First, the substrate was heated at 900 °C for 30 min for cleaning the surface. A thin (~5 nm) BaSi$_2$ template layer was then grown by Ba deposition on the Si substrate at 500 °C for 5 min (reactive deposition epitaxy; RDE). The template was used to control the crystal orientation of the BaSi$_2$ overlayers. An approximately 30-nm-thick Sb-doped n$^+$-BaSi$_2$ layer was grown at 550 °C by MBE for 20 min, to form a TJ with the p$^+$-Si substrate. After that, a 1150-nm-thick undoped n-BaSi$_2$ layer was grown by MBE for 15 h at 600 °C. After the growth, 1-mm-diamter front-surface Au/Cr electrodes were formed by vacuum evaporation and the back-surface Al electrodes by sputtering. For the heterojunction diode, the p-Si substrate ($\rho = 0.1$ Ω·cm) was used. First, a thin BaSi$_2$ template layer was grown by RDE at 500 °C. After that, an approximately 650-nm-thick undoped n-BaSi$_2$ layer was grown by MBE at 600 °C for 590 min. In order to facilitate to make ohmic contacts on the front-surface, another 10-nm-thick Sb-doped n$^+$-BaSi$_2$ layer was grown. To avoid the Sb diffusion into the undoped n-BaSi$_2$ layer, the growth temperature was decreased to 500 °C for the n$^+$-BaSi$_2$ layer. Finally, 0.5-mm-diameter front-surface Al electrodes were formed by sputtering. Backside electrodes were also formed with Al by sputtering. The electrical properties were measured at room temperature (RT).

III. RESULTS AND DISCUSSION

A. Cr/n-BaSi$_2$ Schottky junction diode

Figure 1 shows the *J-V* characteristics of the sample measured at RT. The current increased rapidly as the positive bias was applied to the Au/Cr electrode with respect to the p-Si substrate. Clear rectifying properties were observed in this sample, indicating that the Schottky junction was surely formed on the surface of the thick undoped BaSi$_2$ layers grown on the TJ. The series resistance, R_s, can be deduced from the slope of the $I(dV/dI)$ versus I plot in a large I region, and the shunt resistance, R_{sh}, from the slope of dV/dI at around $V = 0$.[36,37] They were 180 Ω and 1 MΩ, respectively. The logarithmic plot of J with respect to V is inserted in Fig. 1, in which the series resistance and shunt resistance were

subtracted. The reverse saturation current density J_S can be deduced from the intercept of the straight line of the Log(J)-V plot at $V = 0$ and was found to be 6.1×10^{-6} A/cm^2. For a Schottky junction diode, the reverse saturation current density J_S can be expressed by the thermoionic emission theory:[38]

$$J_S = A^* T^2 exp\left(-\frac{q\phi_S}{k_B T}\right), \qquad (1)$$

where A^* is the effective Richardson constant, k_B the Boltzmann constant, $q\phi_S$ the barrier height for electrons in the metal. The $q\phi_S$ was calculated to be 0.73 eV for this Schottky junction. This value is smaller than that predicted from the electron affinity of BaSi$_2$ (3.2 eV) and the work function of Cr (4.5 eV). Thus, a thin interfacial layer is likely to exist between the Cr and the n-BaSi$_2$ due to the oxidation of the BaSi$_2$ surface, and voltages also drop at the interfacial layer.[39,40]

Figure 2(a) shows the $1/C^2$ versus V plot of the Schottky junction diode. The V_D can be deduced by extending the straight line to the voltage axis and it was found to be 0.53 V. The positive ionized donor density, N_D^+, near the surface region of the n-BaSi$_2$ layer, was calculated to be 3×10^{16} cm^{-3} from the C-V characteristics, assuming that the permittivity of BaSi$_2$ approaches 15 for long wavelengths.[11,41] Figure 2(b) shows a simple band diagram of the Cr/n-BaSi$_2$ Schottky junction according to the Schottky-Mott model.[42]

FIG. 2. (a) $1/C^2$ versus V plot of the Schottky junction diode and a line for fitting. (b) Band diagram of the Cr/n-BaSi$_2$ Schottky junction.
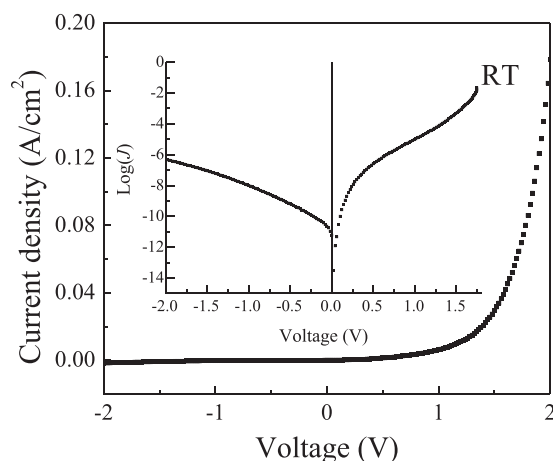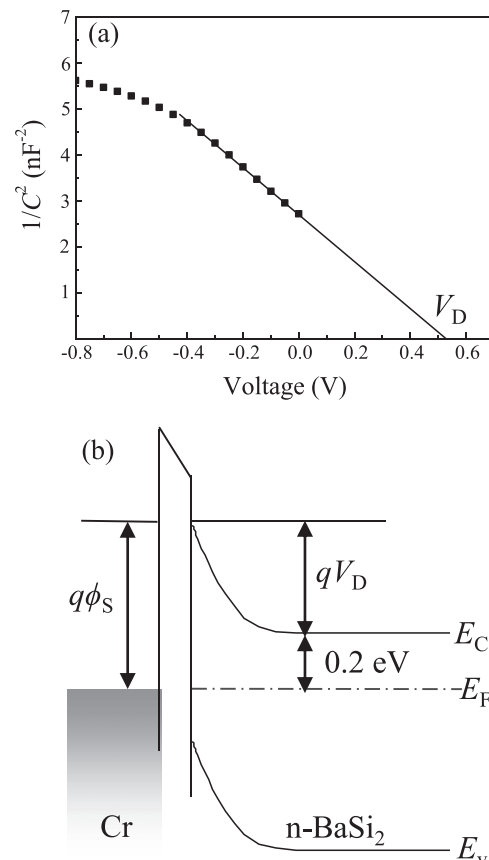

FIG. 1. *J-V* characteristics of the Schottky junction diode measured at RT. The logarithmic plot is inserted. The bias voltage is applied to the Au/Cr electrode with respect to the p-Si substrate.

The E_C-E_F was determined to be 0.2 eV in the n-BaSi$_2$ assuming that it is equal to $q(\phi_S-V_D)$. The electron concentration, n, is given by

$$n = N_C \exp\left(-\frac{E_C - E_F}{k_B T}\right). \qquad (2)$$

Assuming complete ionization of impurity atoms in the n-BaSi$_2$, and thereby $n = N_D^+ = 3 \times 10^{16}$ cm^{-3}, the $E_C - E_F$ was thus calculated to be 0.18 eV at RT. This value is consistent with $q(\phi_S-V_D)$, thereby the band diagram shown in Fig. 2(b).

B. n-BaSi$_2$/p-Si hetero-junction diode

Now let us discuss the electric properties of the n-BaSi$_2$/p-Si heterojunction diode. Figure 3(a) shows the J-V characteristics of the diode measured at RT. The bias voltage was applied to the p-Si substrate with respect to the n$^+$-BaSi$_2$ top layer. Clear rectifying properties were also confirmed in this heterojunction diode. The R_s and R_{sh} were calculated to be 0.8 kΩ and 40 kΩ, respectively. The inserted figure shows the logarithmic plot of J-V characteristics, where the R_s and R_{sh} were subtracted. The ideal factor of the diode, which should be between 1 and 2, was 1.7 under the bias voltages smaller than 0.3 V. However, this value increased to 14.6 when the bias voltage was higher than 0.5 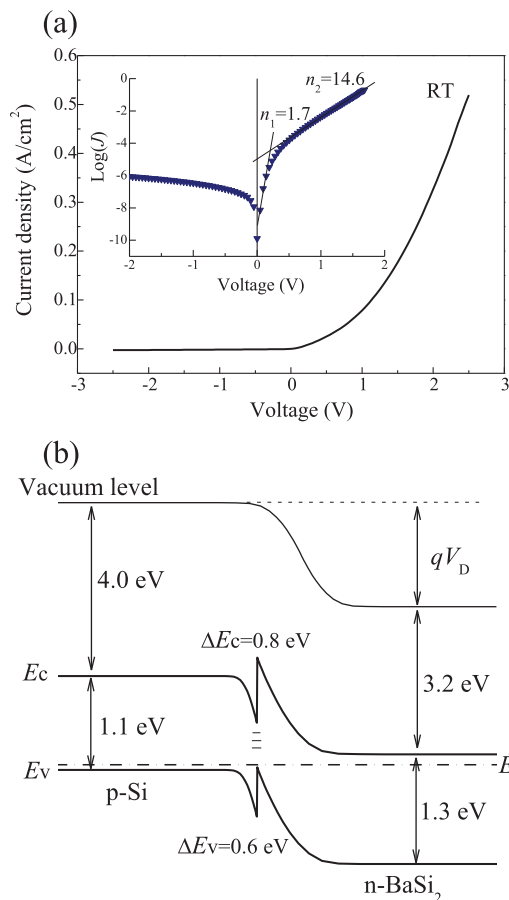V. This might be due to the carrier trapping at the defect states at the interface and a nonlinear series resistance in the diode structure. The reverse saturation current density J_0 was deduced to be 1.2×10^{-4} A/cm^2 from the Log(J) versus V plot in the inserted figure.

Figure 4(a) shows the $1/C^2$ versus V plot of the sample. In our previous works, the electron density in the undoped n-BaSi$_2$ was usually of the order of 10^{16} cm^{-3} from the Hall measurement.[43] This value is smaller by one order of magnitude than that in the p-Si substrate ($p \sim 2 \times 10^{17}$ cm^{-3}) used in this work. Thus, it is reasonable to think that the depletion region extended mostly toward the n-BaSi$_2$ layer. Figure 4(b) shows the n distribution in the n-BaSi$_2$ layer assuming complete ionization of impurity atoms. The average electron density was about 2×10^{16} cm^{-3}. Homogeneous carrier concentration profile indicated the high quality of the BaSi$_2$ epitaxial thin film. As a result, the $1/C^2$ versus V plot was well fitted by a linear broken line as shown in Fig. 4(a). The V_D was deduced to be about 1.5 V in this heterojunction diode. The E_C-E_F is calculated to be 0.19 eV for $n = 2 \times 10^{16}$ cm^{-3} in BaSi$_2$, while the separation of E_F from the top of the valence band, E_V, that is E_F-E_V, is estimated to be 0.10 eV using $p = 2 \times 10^{17}$ cm^{-3} in the p-Si substrate. Thereby, the difference in work function between the n-BaSi$_2$ and p-Si is approximately $4.0 + (1.1 - 0.1) - (3.2 + 0.19) \cong 1.6$ eV. This value is consistent with the experimentally obtained V_D of 1.5 V, as shown in Fig. 4(a).

On the basis of these results on the two kinds of diodes, we conclude that the band diagrams of the undoped n-BaSi$_2$/p-Si and the metal/BaSi$_2$ heterojunctions are well explained by a conventional way widely used in semiconductor physics although BaSi$_2$ is really an unfamiliar

FIG. 3. (a) J-V characteristics of the hetero-junction diode measured at RT. The insertion is the logarithmic plot of J–V characteristics. (b) Band diagram of n-BaSi$_2$/p-Si hetero-junction.

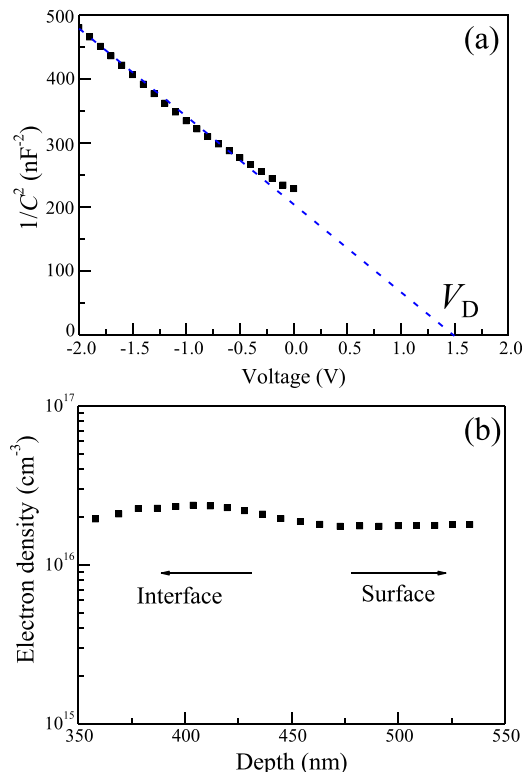
FIG. 4. (a) $1/C^2$ versus V plot and a broken line for fitting (blue). The bias voltage is applied to the p-Si substrate with respect to the n$^+$-BaSi$_2$. (b) Electron density distribution in the BaSi$_2$ layer.

semiconductor material. These results facilitate us to design the device structure of $BaSi_2$ homojunction and heterojunctions solar cells.

IV. CONCLUSIONS

We have formed the Cr/n-$BaSi_2$ Schottky junction and n-$BaSi_2/p$-Si heterojunction diodes. In both samples, clear rectifying properties were observed in the J-V characteristics at RT. In the Schottky junction diode, the J_S was 6.1×10^{-6} A/cm^2, the Schottky barrier height was calculated to be 0.73 eV and the V_D deduced from the $1/C^2$ versus V plot, was found to be 0.53 V. These results were in good agreement with the Schottky-Mott model. In the heterojunction diode, the V_D was found to be 1.5 V, which was well explained by the difference in E_F between the n-$BaSi_2$ and p-Si. The reverse saturation current density was 1.2×10^{-4} A/cm^2. The electron concentrations of the undoped n-$BaSi_2$ layers were of the order of 10^{16} cm^{-3} in both samples from the C-V measurement.

ACKNOWLEDGMENTS

[1]M. A. Green, Prog. Photovolt. Res. Appl. **20**, 472 (2012).
[2]S. Ahmed, K. B. Reuter, O. Gunawan, L. Guo, L. T. Romankiw, and H. Deligianni, Adv. Eng. Mater. **2**, 253 (2012).
[3]B. M. Basol, J. Appl. Phys. **55**, 601 (1984).
[4]M. A. Green and S. R. Wenham, Appl. Phys. Lett. **65**, 2907 (1994).
[5]W. Jaegermann, A. Klein, and T. Mayer, Adv. Mater. **21**, 4196 (2009).
[6]J. Evers, G. Oehlinger, and A. Weiss, Angew. Chem. Int. Ed. **16**, 659 (1977).
[7]M. Imai and T. Hirano, J. Alloys Compd. **224**, 111 (1995).
[8]T. Nakamura, T. Suemasu, K. Takakura, F. Hasegawa, A. Wakahara, and M. Imai, Appl. Phys. Lett. **81**, 1032 (2002).
[9]T. Suemasu, K. Morita, and M. Kobayashi, J. Cryst. Growth **301–302**, 680 (2007).
[10]K. Toh, T. Saito, and T. Suemasu, Jpn. J. Appl. Phys., Part 1 **50**, 068001 (2011).
[11]D. B. Migas, V. L. Shaposhnikov, and V. E. Borisenko, Phys. Status Solidi B **244**, 2611 (2007).
[12]Y. Inomata, T. Nakamura, T. Suemasu, and F. Hasegawa, Jpn. J. Appl. Phys., Part 1 **43**, 4155 (2004).
[13]Y. Inomata, T. Suemasu, T. Izawa, and F. Hasegawa, Jpn. J. Appl. Phys. Part 2 **43**, L771 (2004).
[14]K. Toh, K. O. Hara, N. Usami, N. Saito, N. Yoshizawa, K. Toko, and T. Suemasu, Jpn. J. Appl. Phys., Part 1 **51**, 095501 (2012).
[15]R. Takabe, K. Nakamura, M. Baba, W. Du, M. Ajmal Khan, K. Toko, M. Sasase, K. O. Hara, N. Usami, and T. Sueamsu, Jpn. J. Appl. Phys., Part 1 **53**, 04ER04 (2014).
[16]D. Tsukada, Y. Matsumoto, R. Sasaki, M. Takeichi, T. Saito, N. Usami, and T. Suemasu, Appl. Phys. Express **2**, 051601 (2009).
[17]M. Baba, K. Toh, K. Toko, N. Saito, N. Yoshizawa, K. Jiptner, T. Sekiguchi, K. O. Hara, N. Usami and T. Suemasu, J. Cryst. Growth **348**, 75 (2012).
[18]K. O. Hara, N. Usami, K. Nakamura, R. Takabe, M. Baba, K. Toko, and T. Suemasu, Appl. Phys. Express **6**, 112302 (2013).
[19]R. Takabe, K. O. Hara, M. Baba, W. Du, N. Shimada, K. Toko, N. Usami, and T. Suemasu, J. Appl. Phys. **115**, 193510 (2014).
[20]M. Kobayashi, Y. Matsumoto, Y. Ichikawa, D. Tsukada, and T. Suemasu, Appl. Phys. Express **1**, 051403 (2008).
[21]M. Ajmal Khan, T. Saito, K. Nakamura, M. Baba, W. Du, K. Toh, K. Toko, and T. Suemasu, Thin Solid Films **522**, 95 (2012).
[22]M. Ajmal Khan, K. O. Hara, W. Du, M. Baba, K. Nakamura, M. Suzuno, K. Toko, N. Usami, and T. Suemasu, Appl. Phys. Lett. **102**, 112107 (2013).
[23]R. Takabe, M. Baba, K. Nakamura, W. Du, M. A. Khan, S. Koike, K. Toko, K. O. Hara, N. Usami, and T. Suemasu, Phys. Status Solidi C **10**, 1753 (2013).
[24]K. O. Hara, Y. Hoshi, N. Usami, Y. Shiraki, K. Nakamura, K. Toko, and T. Suemasu, Thin Solid Films **557**, 90 (2014).
[25]K. O. Hara, Y. Hoshi, N. Usami, Y. Shiraki, K. Nakamura, K. Toko, and T. Suemasu, Thin Solid Films **534**, 470 (2013).
[26]K. O. Hara, N. Usami, Y. Hoshi, Y. Shiraki, M. Suzuno, K. Toko, and T. Suemasu, Jpn. J. Appl. Phys., Part 1 **50**, 121202 (2011).
[27]K. Nakamura, M. Baba, M. Ajmal Khan, W. Du, M. Sasase, K. O. Hara, N. Usami, K. Toko, and T. Suemasu, J. Appl. Phys. **113**, 053511 (2013).
[28]K. Nakamura, K. Toh, M. Baba, K. M. Ajmal, W. Du, K. Toko, and T. Suemasu, J. Cryst. Growth **378**, 189 (2013).
[29]N. Zhang, K. Nakamura, M. Baba, K. Toko, and T. Suemasu, Jpn. J. Appl. Phys., Part 1 **53**, 04ER02 (2014).
[30]T. Suemasu, K. Morita, M. Kobayashi, M. Saida, and M. Sasaki, Jpn. J. Appl. Phys., Part 2 **45**, L519 (2006).
[31]B. E. Umirzakov, D. A. Tashmukhamedova, E. U. Boltaev and A. A. Dzhurakhalov, Mater. Sci. Eng. B **101**, 124 (2003).
[32]W. Du, T. Saito, M. Ajmal Khan, K. Toko, N. Usami, and T. Suemasu, Jpn. J. Appl. Phys., Part 1 **51**, 04DP01 (2012).
[33]T. Saito, Y. Matsumoto, M. Suzuno, M. Takeishi, R. Sasaki, N. Usami, and T. Suemasu, Appl. Phys. Express **3**, 021301 (2010).
[34]T. Suemasu, T. Saito, K. Toh, A. Okada, and M. Ajmal Khan, Thin Solid Films **519**, 8501 (2011).
[35]W. Du, M. Suzuno, M. Ajma Khan, K. Toh, M. Baba, K. Nakamura, K. Toko, N. Usami, and T. Suemasu, Appl. Phys. Lett. **100**, 152114 (2012).
[36]H. Norde, J. Appl. Phys. **50**, 5052 (1979).
[37]S. K. Cheung and N. W. Cheung, Appl. Phys. Lett. **49**, 85 (1986).
[38]F. A. Padovani and R. Stratton, Solid-State Electron. **9**, 695 (1966).
[39]S. M. Sze, *Physics of Semiconductor Devices*, 3rd ed. (Wiley, New York, 1981), p. 140.
[40]A. M. Cowley and S. M. Sze, J. Appl. Phys. **36**, 3212 (1965).
[41]N. A. A. Latiff, T. Yoneyama, T. Shibutami, K. Matsumaru, K. Toko, and T. Sueamsu, Phys. Status Solidi C **10**, 1759 (2013).
[42]N. F. Mott, Proc. Camb. Philos. Soc. **34**, 568 (1938).
[43]K. Morita, Y. Inomata, and T. Suemasu, Thin Solid Films **508**, 363 (2006).